Analysis of the Stability of Hemoglobin S Double Strands

Xiang-Qi Mu,*# Lee Makowski,# and Beatrice Magdoff-Fairchild*
*Hemotology Division, Medical Service, St. Luke's-Roosevelt Hospital Center and Department of Medicine, College of Physicians and Surgeons of Columbia University, New York, New York 10025, and #Institute of Molecular Biophysics, Florida State University, Tallahassee, Florida 32306 USA

ABSTRACT The deoxyhemoglobin S (deoxy-HbS) double strand is the fundamental building block of both the crystals of deoxy-HbS and the physiologically relevant fibers present within sickle cells. To use the atomic-resolution detail of the hemoglobin-hemoglobin interaction known from the crystallography of HbS as a basis for understanding the interactions in the fibers, it is necessary to define precisely the relationship between the straight double strands in the crystal and the twisted, helical double strands in the fibers. The intermolecular contact conferring the stability of the double strand in both crystal and fiber is between the β6 valine on one HbS molecule and residues near the EF corner of an adjacent molecule. Models for the helical double strands were constructed by a geometric transformation from crystal to fiber that preserves this critical interaction, minimizes distortion, and makes the transformation as smooth as possible. From these models, the energy of association was calculated over the range of all possible helical twists of the double strands and all possible distances of the double strands from the fiber axis. The calculated association energies reflect the fact that the axial interactions decrease as the distance between the double strand and the fiber axis increases, because of the increased length of the helical path taken by the double strand. The lateral interactions between HbS molecules in a double strand change relatively little between the crystal and possible helical double strands. If the twist of the fiber or the distance between the double strand and the fiber axis is too great, the lateral interaction is broken by intermolecular contacts in the region around the β6 valine. Consequently, the geometry of the β6 valine interaction and the residues surrounding it severely restricts the possible helical twist, radius, and handedness of helical aggregates constructed from the double strands. The limitations defined by this analysis establish the structural basis for the right-handed twist observed in HbS fibers and demonstrates that for a subunit twist of 8°, the fiber diameter cannot be more than ~300 Å, consistent with electron microscope observations. The energy of interaction among HbS molecules in a double strand is very slowly varying with helical pitch, explaining the variable pitch observed in HbS fibers. The analysis results in a model for the HbS double strand, for use in the analysis of interactions between double strands and for refinement of models of the HbS fibers against x-ray diffraction data.

INTRODUCTION

Sickle-cell anemia is caused by a mutation that replaces a glutamate at position 6 of the β-chain of normal hemoglobin (HbA) with a valine in sickle-cell hemoglobin (HbS). This mutation plays an important role in the aggregation of deoxygenated HbS molecules in erythrocytes and ultimately causes the symptoms associated with sickle-cell anemia. The crystal structure of deoxy-HbS (Wishner et al., 1975; Padlan and Love, 1985a) revealed that the HbS molecules are arranged in the crystal as half-staggered double strands. The lateral molecular contacts between single strands within a double strand involve the interaction of Val^6 in the A helix of the β_2 chain in one HbS molecule with residues in the E and F helices and EF corner of the β_1 chain in an adjacent molecule. In this paper those contacts are referred to as β6 contacts. Comparison of the refined structure of HbS with that of HbA (Padlan and Love, 1985a) demonstrated that the intermolecular interaction involving the β6 valine is accommodated by a bend in the A helix of which it is a part. Without this distortion, close contacts around β6 valine would prevent a stable intermolecular interaction.

The structure of the deoxy-HbS fiber comprises seven half-staggered double strands that twist around one another with an average helical pitch of ~2900 Å (Dykes et al., 1979; Carragher et al., 1988). The three-dimensional reconstructions obtained by Edelstein and by Josephs agree on the overall architecture of the HbS fibers, but differ in important details. Ambiguity in the scaling of electron micrographs has led to substantial discussion about the packing density within the fibers (Cretegny and Edelstein, 1993; Watowich et al., 1993).

In addition to the physiological relevant fiber made up of seven double strands, a variety of other polymorphic assemblies have been reported, including different crystal forms (Wishner et al., 1975; Rosen and Magdoff-Fairchild, 1982; Magdoff-Fairchild et al, 1982), macrofibers (Potel et al., 1984; Bluemke et al., 1988), twisted crystals (Wellems and Josephs, 1980), paracrystals (Bluemke et al., 1988), and fascicles (McDade et al., 1989). Except for some of the single crystals, all observed assemblies appear to be lateral aggregates of double strands with different pitches and radii (Makowski and Magdoff-Fairchild, 1986).

The similarity of x-ray diffraction patterns from HbS fibers and HbS single crystals provides strong evidence that the molecular arrangements in the fibers and the crystals are very closely related (Magdoff-Fairchild and Chiu, 1979). It

Received for publication 7 May 1997 and in final form 24 September 1997.
Address reprint requests to Dr. Lee Makowski, Institute of Molecular Biophysics, Florida State University, Tallahassee, FL 32306. Tel.: 904-644-0451; Fax: 904-561-1406; E-mail: makowski@sb.fsu.edu.

0006-3495/98/01/655/14 $2.00

follows that the double strand is very similar in the two structures. The correspondence of the x-ray diffraction patterns from crystals and from fibers provides a basis for the modeling of intermolecular interactions in HbS fibers, based on the atomic coordinates obtained by x-ray crystallographic studies of crystalline HbS. However, the helical twist of the double strands in the HbS fibers (DSFs) precludes an arrangement identical to that of the straight double strands in the crystals (DSXs). Transformation of a DSX into a DSF requires distortion of the DSX, as shown in Fig. 1 where Fig. 1 *a* is a DSX, Fig. 1 *b* is a central DSF in which the single strands twist around the fiber axis, and Fig. 1 *c* is a noncentral DSF, in which the single strands twist around a helix, which in turn twists around the fiber axis.

The correspondence between the x-ray diffraction patterns from crystals and fibers indicates that the axial distance between HbS molecules in each single strand is identical for all double strands, regardless of radius. As shown in Fig. 1, when reference molecules of every HbS double strand are located at the same height (as indicated by the *broken lines at the bottom*), the successive molecules along the strand are all at the position of the third broken line, 64 Å above the bottom. This is also the condition for the preservation of contacts among double strands (Magdoff-Fairchild and Chiu, 1979). If each double strand in the fiber had a different axial periodicity, there would be no regular pattern of interactions among them, and a stable fiber would not form. As can be seen in Fig. 1, the immediate consequence of this is that the spacing of HbS molecules along their helical path in a single strand in the fiber must be larger than that along their straight path in the crystal. The intermolecular spacing along the helical single strands in Fig. 1 *c* must thereby be larger than the corresponding spacing along the straight single strands in Fig. 1 *a*. This effect increases with increasing radius of the DSFs.

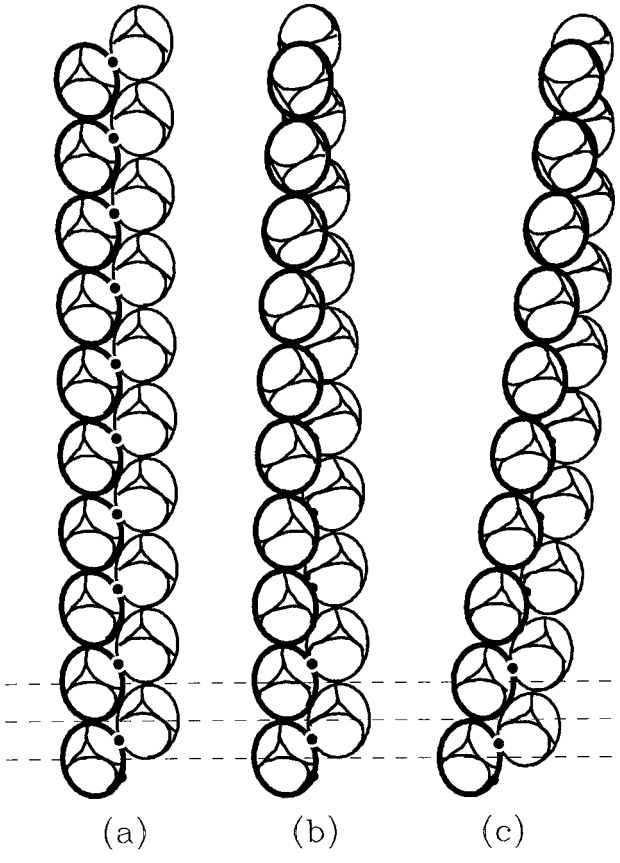

FIGURE 1 (*a*) HbS double strand in the crystal. (*b*) Central DSF, an HbS helical double strand with the fiber axis going through between the two strands. (*c*) Noncentral DSF, an HbS helical double strand with 85 Å as the distance from the fiber axis. The subunit twist for *b* and *c* is 8°. The HbS molecule is represented by an ellipse. The regions of four chains within the molecule are marked by demarcation curves. The molecular rotations may be recognized by changes in these curves. β6 contact, the lateral intermolecular interaction within HbS double strands, is represented by a black spot. The first and the third broken lines go through the molecular centers of two successive HbS molecules along a single strand in DSX, and perpendicular with DSX. The middle broken line goes through the molecular center of the lateral adjacent molecule within the DSX, and parallel with the other two lines. DSFs in *b* and *c* were constructed using method in this paper.

When an HbS molecule is translated to the position of a successive neighbor along the HbS strand, it has to be rotated about the molecular axis by an angle equal to the subunit twist of the fibers. This is required by the symmetry of the fibers and can be seen in Fig. 1. The four chains of an HbS molecule are indicated by demarcation curves on the molecular surfaces in that figure. The changes of molecular rotation along HbS double strands are indicated by variations in the demarcation curves in Fig. 1, *b* and *c*.

The transformation from DSX into DSF must occur without severance of the β6 interaction that provides the stability for the double strands. The first consequence of this requirement is that the relative height of two lateral neighbor molecules within a noncentral double strand has to be changed. As shown in Fig. 1 *c*, the lateral neighbor of the reference molecule of a noncentral DSF is lower than that in a DSX or in a central DSF. The second consequence is that each HbS molecule has to be tilted with respect to the fiber axis as the helical path is, to preserve the intermolecular interactions as much as possible. The third consequence is that the relative molecular rotation between the two lateral neighbor molecules along a DSF also has to be changed, compared to that in a DSX. This change is too small to be observed in Fig. 1. In the geometric transformation described below, the double strands are distorted so as to maintain the β6 interaction and to conform to the helical symmetry of the fiber while at the same time distorting the geometry of the double strand as little as possible from its structure in the crystal.

Edelstein transformed a DSX into the central DSFs by rotations and inclinations, or tilts, of HbS molecules (1981). Cretegny and Edelstein (1993) constructed HbS fiber models using a method in which all seven DSFs were formed simply by rotations and tilts of the HbS molecules of the DSX. However, for a noncentral DSF, this transformation results in the two lateral intermolecular distances for a noncentral DSF being nonequivalent. One lateral distance may be too large to make any intermolecular interaction, whereas at the same time the other may be impossibly short. In other

words, the $\beta 6$ contacts cannot be preserved by a transformation of this kind. Furthermore, potential intermolecular penetrations will occur in fibers transformed in this way.

Watowich et al. (1989, 1993) paid great attention to constraining the distance between lateral adjacent molecules within HbS double strands during the transformation from crystal into fiber. They implemented this constraint by fixing the molecular distance in the plane normal to the helical path to be 46 Å. For higher resolution modeling, however, the center-to-center distance should be fixed instead. The reason for this is as follows: Double strands at higher radii are stretched relative to those at lower radii because they follow a longer helical path (as seen in Fig. 1). For the $\beta 6$ contact to be maintained in the DSFs at higher radius, the distance between single strands in the plane normal to the helical path must decrease. Otherwise, the $\beta 6$ contact will be changed due to variation of molecular distance. The method used by Watowich et al. may not seriously affect the comparison of molecular models with a low-resolution three-dimensional reconstruction from electron microscopy, but may not be used for counting of residues contributing to contacts or for calculation of intermolecular interaction energy as described here. In this work, the center-to-center lateral molecular distance within the HbS double strand has been fixed to be 56 Å.

In this paper we present a systematic analysis of the geometric transformation of straight HbS double strands as they occur in a crystal into the helical double strands found in HbS fibers. A method is described for carrying out this transformation while preserving the $\beta 6$ interaction and minimizing all distortions to the double strand. This method is then used to calculate the intermolecular interactions among HbS molecules in double strands with a wide range of structural parameters. The range of allowable structural parameters for double strands is defined from this work. The calculations demonstrate that the conditions required for the stability of DSFs highly restrict the radius of HbS fibers, their handedness, the orientation of the molecular axes of the HbS molecules in the fibers, and the length of the axial repeat distance of HbS fibers.

METHODS

Restraints on the transformation of DSX to DSF

Padlan and Love (1985b) analyzed in detail the molecular contacts in the deoxy-HbS crystal structure, refined at a resolution of 3.0 Å (Padlan and Love, 1985a), and compared them with those in crystals of deoxy-HbA, deoxy-HbC, and deoxy-HbF. Two sets of axial molecular contacts in deoxy-HbS crystal are very similar to those in the other three structures. However, the lateral molecular contacts between deoxyhemoglobin single strands in HbS were not observed in any of the others where no double strands were formed. The quaternary structure of deoxy-HbS is almost identical to those of deoxy-HbA and deoxy-HbC (orthorhombic form). The only significant differences in the tertiary structures of the chains among these hemoglobin molecules is a hingelike shift of the A helices of the β_2 chain in the HbS molecule. Without these shifts the lateral contacts between the single strands in the DSX would be precluded by molecular interactions adjacent to Val $\beta 6$.

Extensive experimental studies suggest that the lateral intermolecular contacts, or the $\beta 6$ contact, within the HbS double strand are almost the same for the crystal and for the fiber (Eaton and Hofrichter, 1990). In addition to the necessary molecular inclinations in DSF (Edelstein, 1981), two more geometric conditions are necessary for the preservation of the $\beta 6$ contact along the entire double strand. First, the lateral intermolecular distances (corresponding to the $\beta 6$ contacts) should be the same for the DSX and for any DSF in the HbS fibers. Second, the relative orientations between the two molecules interacting through the $\beta 6$ contact should be half of the subunit (one subunit = two HbS molecules) twist, i.e., 0.5 ω.

The x-ray diffraction pattern of an HbS fiber displays a series of sharp meridional reflections (Magdoff-Fairchild and Chiu, 1979). The repeat distance along the fiber axis was obtained from the spacings in this pattern. At 64 Å, it is very close to the unit cell parameter, a (63.3 Å), in the crystalline HbS (Wishner et al., 1975). Consequently, any possible model for the DSF has to satisfy the constraint that the subunit rise along the fiber axis is 64 Å.

From these considerations, the restraints on the transformation of DSX to DSFs that were assumed in this work were

1. The deoxy-HbS molecules are rigid during the transformation.
2. The lateral molecular distances ($\beta 6$ contact distances) are held fixed.
3. The relative orientation between lateral adjacent molecules is half of the subunit twist.
4. The subunit rise along the fiber axis is always equal to 64 Å.

Structural parameters of DSX

A DSX is drawn schematically in the fiber reference system in Fig. 2. The fiber axis is chosen as the X axis. A molecule in the double strand is designated by the character S or T, denoting one of the two molecular strands, with a subscript to indicate its position along the strand. Creation of the fiber double strand involves adjustments of the molecular orientations, shifts of S_0 and T_0 from their positions in the DSX to their positions in the DSFs, and the generation of other molecules of the DSF by the rotation of S_0 and T_0 by the subunit twist and translation by the subunit rise. A successful transformation will produce viable molecular interactions along the entire double strand. There are four distinct interactions in a double strand; two lateral, S_0-T_0 and S_0-T_{-1}; and two axial, S_0-S_1 and T_0-T_1. Accordingly, there are four independent molecular distances, d_1, d_2, d_3, and d_4.

In addition to the subunit twist ω, we need two more parameters to define a subunit of DSX. They are, as shown

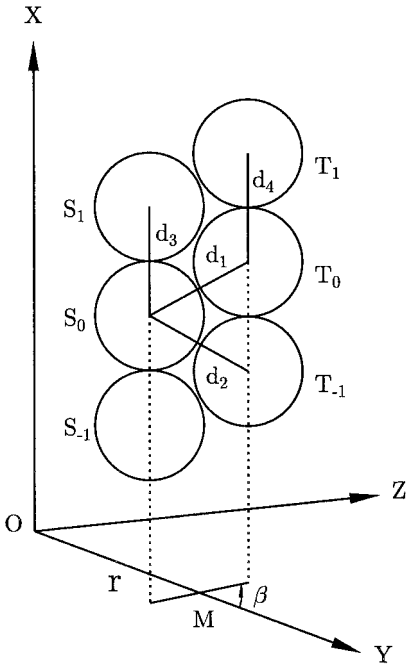

FIGURE 2 A double strand, composed of deoxygenated sickle cell hemoglobin molecules, in the untwisted state as in the crystal, but drawn in the fiber reference system. The repeating unit of the double strand contains two molecules, S_0 and T_0. The fiber axis is taken as the X axis of the system. The Y axis goes through point *M*, the projection of the mass center of the double strand onto the *YOZ* plane. The Z axis is chosen to make the system right-handed. *r*, equal to *OM*, is defined as the radius of the double strand. The angle β is defined as the angle between the Y axis and the projection of the line connecting molecules S_0 and T_0. There are four independent molecular distances: $d_1 = S_0$–T_0, $d_2 = S_0$–T_{-1}, $d_3 = S_0$–S_1, and $d_4 = T_0$–T_{-1}.

in Fig. 2, the distance between the mass center of the DSX and the fiber axis, and β, the angle between the line connecting the mass center and the fiber axis and the projection of the line connecting S_0 and T_0. It will be shown that the intermolecular interactions within a DSF are β independent in most cases.

Another parameter that was initially taken into consideration in our study of the intermolecular interactions within DSFs is the difference between the molecular orientations of an HbS molecule in a DSX and that in a DSF. Energy calculations for DSFs with a wide variety of fiber twists, radii, and angle β were carried out (see below). These results indicated that the relative rotation between an HbS molecule in a DSX and in a DSF that corresponds to an energy minimum for the DSF is obtained only when the relative orientation between molecule T_0 in DSX and T_0 in DSF is $-0.1\ \omega$ (ω is the subunit twist)—less than a 1° rotation for all viable fibers. As a result of these calculations, this relative orientation was not considered a variable parameter for the remainder of this work.

In deoxy-HbS crystals the double strand has an approximate twofold axis; that is, the repeating unit of the DSX is a pair of molecules related to one another by a pseudo-2_1 axis. It is not clear whether the molecular interactions in the crystal represent the low-energy state of the double strand or if a closely related double strand with perfect 2_1 symmetry would have a lower free energy but is not observed because of crystal contacts. Consequently, we have chosen to carry out calculations based on both the observed crystalline double strand, DSX, and on a hypothetical double strand, constructed computationally to have exact 2_1 symmetry. The calculations described below were carried out for both of these models, by the same method.

DSF construction

The procedure of transformation of DSX with structural parameters of $\omega = 8°$, $r = 85$ Å, and $\beta = 90°$ into DSF is shown in Fig. 3. The mass centers of molecules S_0, T_0, and S_1 of the DSX are marked as s_0, t_0, and s_1, respectively, in the fiber reference system *XYZ*, as shown in Fig. 3 *a*. They are shifted to new positions s_0, t_0'', and s_1' after the transformation, as shown in Fig. 3 *b*. It is straightforward to calculate the coordinates of point s_1', the new position for molecule S_1, whereas s_0, the mass center of molecule S_0, is fixed for convenience. As mentioned above, t_0'' should be equidistant from s_0 and s_1. There are infinite solutions for t_0'' in a three-dimensional space. Only one that keeps the distance between T_0 and the fiber axis unchanged or changed to a minimum extent is chosen as the final solution. The calculation is outlined in the Appendix.

A deformed HbS double strand is constructed on plane *xoy* of a local reference system *xyz* as follows, as shown in Fig. 3 *c*. The origin of the system is located at the mass center of molecule S_0, and its axes are parallel with those of the fiber system. The intermolecular distances within the deformed double strand are the same as those in Fig. 3 *b*. The relative orientation between molecule S_0 and S_1 is equal to the subunit twist ω; that between S_0 and T_0 is equal to half the twist, $0.5\ \omega$. The points s_0, t_0'', and s_1' in Fig. 3 *b* may be translated to the local reference system, with s_0 coinciding with the origin. They compose a target of the transformation. The deformed double strand is then rotated as a rigid body by three Eulerian angles, so that the mass centers of three molecules coincide with three points of the target. After the rotations molecules S_0 and T_0 compose the subunit of the DSF corresponding to the parameters ω, *r*, and β.

The subunit is moved back to the fiber reference system and is imposed by the fiber symmetry to generate the whole double strand.

Energy calculations

Energy calculations were carried out by the method of Wodak and Janin (1978). The intermolecular energy of interaction between proteins in solution may be approximated by the sum of hydrophobic bond energy and the nonbonded van der Waals energy (Wodak and Janin, 1978). Other energy terms, like hydrogen bond and electrostatic interaction, contribute very little because they are almost the

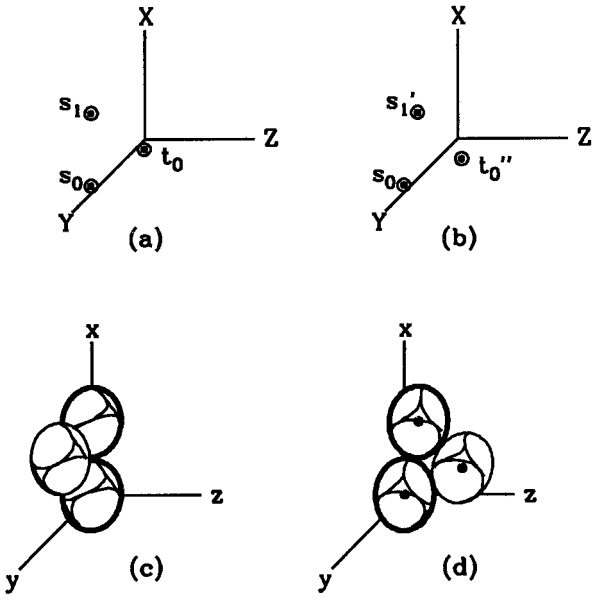

FIGURE 3 Transformation of DSX into DSF. (*a*) Starting positions of three representing molecules of an HbS double strand in the fiber reference system *XYZ*. s_0, t_0, and s_1 are mass centers of molecules S_0, T_0, and S_1 of DSX, with parameters $\omega = 8°$, $r = 85$ Å, and $\beta = 90°$. (*b*) New positions of three molecules after the transformation of the DSX into DSF in the same reference system. s_0 is fixed during the transformation for convenience. The molecular distance between t_0'' and s_1' is equal to that between t_0'' and s_0. The distance between molecule T_0 and the fiber axis is fixed during the transformation in most cases. A small adjustment (no larger than 0.4 Å) for this distance has to be made when r and/or ω is large and β is close to 0° or 180°. (*c*) Creation of a deformed double strand. *xyz* represents a local reference system with its origin located at s_0 and axes parallel with those of the fiber system. Molecules S_0, T_0, and S_1 are placed at the origin, axis *ox*, and on plane *xoy*, respectively. Intermolecular distances are the same as those between points s_0, t_0'', and s_1' in *b*. The relative molecular orientation between S_0 and S_1 is equal to the subunit twist ω, and that between T_0 and S_0 is half of the twist, 0.5 ω. The deformed HbS double strand, comprising these molecules, involves structural information about the relative positions and relative orientations in the DSF, transformed from DSX with parameters $\omega = 8°$, $r = 85$ Å, and $\beta = 90°$. (*d*) Rotations of the deformed double strand. The points s_0, t_0'', and s_1' in *b* are translated as a rigid body in the local reference system *xyz*, where s_0 coincides with the origin. These points, marked with black spots in the figure, compose a target for the transformation. The deformed double strand is then rotated by three Eulerian angles as a rigid body, so that the mass centers of three molecules coincide with three points of the target. The molecules S_0 and T_0 after these rotations comprise the subunit of the DSF, corresponding to parameters ω, r, and β.

same for the protein-protein interactions as they are for protein-solvent interactions. To estimate the protein-protein interaction energy, a simplified protein model is used in which each residue is represented by a sphere centered on its side-chain centroid (α-carbon atom included), and all of the atomic interactions are replaced by interactions among these spheres (Levitt, 1976; Wodak and Janin, 1978).

This model has been applied by Janin and co-workers to predict the structure of a protein-protein complex between the β-lactamase TEM-1 and the β-lactamase inhibitory protein (BLIP) in a complicated docking procedure. They correctly deduced the general mode of binding of the 165-amino acid inhibitor (BLIP) to the 262 amino acid enzyme (TEM-1 β-lactamase), as did five other research groups for the same complex, using different docking programs and more detailed descriptions for protein molecules (Strynadka et al., 1996).

Neglecting hydrogen and ionic bonds in the energy calculation should work particularly well for the molecular interactions within HbS double strands, because the molecular interactions in the HbS crystal are predominated by hydrophobic and van der Waals-type interactions (Padlan and Love, 1985b). The first lateral contact, the S_0-T_0 contact, involves 37 atom pairs, with only one potential hydrogen bond and no ion pair interactions. In the 72 atom pairs in the second lateral contact, or S_0-T_{-1} contact, there are only four potential hydrogen bonds and one ion pair. The first axial contact (S_0-S_1 contact) involves 51 atom pairs with one potential hydrogen bond and no ion pairs; and in the 58 atom pairs involved in the second axial contact (T_0-T_1 contact), there are only four potential H-bonds.

The hydrophobic bond energy comes from the reduction of accessible surface area (ASA) of residues when protein molecules interact. ASAs were calculated using an analytical approximation formula (Wodak and Janin, 1980), with a factor of 47 cal/mol/Å^2 to convert the ASA to free energy (Sharp et al., 1991). The simplified protein model of HbS was constructed from the atomic coordinates of the refined deoxy-HbS crystal structure at 3.0-Å resolution, as deposited in the Protein Data Bank (Padlan and Love, 1985a; Bernstein et al., 1977). The spherical radii of the 20 residues were taken from Levitt (1976).

For a DSX, the resulting intermolecular energies were calculated to be S_0-T_0, −42.33 kcal/dimer; S_0-T_{-1}, −47.97 kcal/dimer; S_0-S_1, −29.85; T_0-T_1, −32.37 kcal/dimer. The lateral and the axial energies are −90.20 kcal/dimer and −62.22 kcal/dimer, respectively. The total energy change for formation of a DSX is −152.41 kcal/dimer. Note that the contacts associated with the largest energy changes are the two β6 (lateral) contacts.

RESULTS AND DISCUSSION

The polymorphism of HbS aggregates (Makowski and Magdoff-Fairchild, 1986) indicates that the double strand may exist over a wide range of parameters r, ω, and β. Consequently, DSXs were transformed into DSFs for a very wide range of parameters. For comparison, the hypothetical straight double strand, comprising two HbS molecules related by a real 2_1 symmetry, were transformed into a helical double strand, also for a wide range of parameters. In both cases, helical double strands were constructed for radii r from 0 to 200 Å in steps of 10 Å, subunit twist ω from −10° to 10° in steps of 1°, and β from 0° to 360° in steps of 10°. A wider range of parameters was covered for the transformation of DSX into DSF. The radius r was extended to 400 Å, 500 Å, 700 Å, 840 Å, and 1050 Å for $\omega = 2°$, 1.5°, 1.0°, 0.8°, and 0.6°, respectively; angle β varied from 0° to 360°

in steps of 10° for each set of r and ω. A total of 50,000 DSF models were examined. In addition to all DSFs observed in various aggregates of HbS molecules, many of them are unknown or hypothetical.

Every DSF model has been scored by associated energies, including two lateral interactions and two axial, within the double strand. As shown later, when transformed from DSX, all observed DSFs have high scores, whereas those with very low scores have never been observed.

The energies calculated by the Wodak-Janin technique provided not only scores for DSF models, but also information about structural properties of the intermolecular interactions within DSF.

In the three-dimensional parameter space of the DSF models, there is a low-energy region where the total interaction energies within a DSF are equal to or very close to that of a DSX. The energies in other parts of the space are much higher. In the low-energy region, the energies within the DSF are nearly independent of the angle β. Consequently, we may conveniently analyze this region with a two-dimensional map, exploring dependence on r and ω, and ignoring β. Outside this region the energies are both high and very β dependent.

Intermolecular energies within a DSF

The total interaction within a DSF in the low-energy region was averaged over the whole range of β, from 0° to 360°, for every parameter set of r and ω, and standard deviations were calculated. When the energy is lower than −106 kcal, or 70% of the energy of a DSX, the standard deviation is not larger than 4 kcal. As shown in Table 1, the standard deviation is usually less than 1% of the mean for radii from 0 to 100 Å and for a subunit twist from −3° to 8°, with a few exceptions, where the standard deviation is less than 2% of the mean. This confirms that the molecular interactions within the DSF are β-independent over wide ranges of r and ω.

It is shown in Table 1 that the energies are also insensitive to the radius r. When $\omega = 8°$, the energy is almost a constant for $r = 0–40$ Å, and only changes gradually for larger r. The energy coefficient is as small as 0.33 kcal/Å for noncentral DSFs, where r is 30–100 Å. The major factor in the energy dependence on radius of the double strand in these ranges of parameters is the stretching of the strand at progressively larger radii. For a radii of 100 Å and a subunit twist of 8°, the axial interaction distance s_0s_1 has increased from 64 Å to 65.5 Å.

TABLE 1 The interaction energies within HbS double strands*#

r/Å	0	10	20	30	40
ω/° = −4	−100.0	−100.4 ± 0.3	−100.5 ± 0.7	−100.4 ± 1.2	−100.2 ± 1.8
−3	−134.0	−133.9 ± 0.1	−133.6 ± 0.2	−133.6 ± 0.4	−133.4 ± 0.3
−2	−148.3	−148.3 ± 0.0	−148.1 ± 0.1	−148.0 ± 0.1	−147.7 ± 0.1
−1	−152.9	−152.8 ± 0.1	−152.7 ± 0.1	−152.7 ± 0.1	−152.7 ± 0.1
0	−152.4				
1	−151.8	−151.8 ± 0.0	−151.8 ± 0.0	−151.8 ± 0.0	−151.7 ± 0.0
2	−148.9	−148.8 ± 0.0	−148.8 ± 0.0	−148.7 ± 0.0	−148.3 ± 0.3
3	−146.9	−147.0 ± 0.3	−147.0 ± 0.3	−146.7 ± 0.3	−146.3 ± 0.3
4	−146.4	−146.1 ± 0.3	−146.0 ± 0.1	−145.6 ± 0.0	−144.8 ± 0.3
5	−145.3	−145.3 ± 0.1	−145.1 ± 0.2	−144.4 ± 0.2	−143.8 ± 0.5
6	−144.1	−144.2 ± 0.3	−143.8 ± 0.3	−143.2 ± 0.5	−142.2 ± 0.5
7	−142.3	−142.3 ± 0.2	−141.7 ± 0.3	−140.9 ± 0.4	−139.4 ± 0.4
8	−140.2	−140.2 ± 0.5	−139.7 ± 0.4	−139.3 ± 0.7	−138.3 ± 0.8
9	−137.6	−136.9 ± 0.3	−136.4 ± 0.4	−134.8 ± 0.3	−132.9 ± 1.0
10	−131.1	−130.7 ± 0.3	−129.5 ± 0.6	−127.3 ± 0.9	−124.7 ± 1.9

50	60	70	80	90	100
−100.0 ± 2.0	−99.4 ± 2.2	−98.4 ± 2.4	−96.9 ± 2.5	−94.4 ± 2.3	−91.2 ± 2.4
−133.1 ± 0.4	−132.5 ± 0.5	−131.7 ± 0.5	−130.9 ± 0.6	−129.7 ± 0.7	−128.3 ± 0.8
−147.4 ± 0.2	−147.0 ± 0.2	−146.6 ± 0.2	−146.4 ± 0.5	−146.1 ± 0.6	−145.7 ± 0.6
−152.6 ± 0.1	−152.5 ± 0.1	−152.4 ± 0.1	−152.3 ± 0.1	−152.2 ± 0.1	−152.0 ± 0.1
−151.6 ± 0.0	−151.6 ± 0.0	−151.5 ± 0.0	−151.4 ± 0.0	−151.3 ± 0.0	−151.2 ± 0.0
−148.1 ± 0.3	−147.8 ± 0.3	−147.6 ± 0.2	−147.2 ± 0.2	−146.9 ± 0.3	−146.4 ± 0.3
−145.8 ± 0.3	−145.2 ± 0.3	−144.6 ± 0.3	−144.0 ± 0.6	−143.3 ± 0.6	−142.6 ± 0.6
−144.1 ± 0.5	−143.3 ± 0.7	−142.3 ± 0.8	−141.0 ± 0.5	−139.6 ± 0.5	−138.1 ± 0.4
−142.7 ± 0.7	−141.3 ± 0.6	−139.7 ± 0.5	−137.9 ± 0.4	−136.1 ± 0.4	−134.5 ± 0.4
−140.8 ± 0.4	−138.8 ± 0.5	−136.8 ± 0.5	−134.4 ± 0.4	−132.0 ± 0.5	−129.1 ± 1.0
−137.6 ± 0.3	−135.9 ± 0.8	−133.7 ± 0.6	−131.1 ± 0.4	−128.5 ± 1.0	−124.8 ± 1.3
−136.2 ± 0.8	−133.1 ± 1.1	−129.8 ± 1.3	−126.4 ± 2.0	−121.4 ± 2.0	−116.1 ± 1.9
−130.1 ± 1.4	−126.4 ± 1.5	−122.8 ± 1.8	−117.7 ± 2.0	−112.1 ± 2.1	−105.8 ± 2.2
−120.7 ± 2.3	−116.1 ± 2.3	−110.8 ± 2.3	−105.1 ± 2.7	−98.1 ± 2.9	−89.8 ± 3.7

*The energy includes two lateral and two axial interactions.

#The energy is averaged over the whole range of β (0° to 360°).

This decreases the number of residues involved in the axial contact, and decreases the interaction energy.

Handedness of DSF

The energies, averaged over the whole range of angle β, 0° to 360°, in a wider range of r and ω, are shown in Fig. 4 *a*, where five energy levels, $0.9E_x$, $0.8E_x$, $0.7E_x$, $0.6E_x$, and $0.5E_x$ (where E_x is the total intermolecular interaction energy for a DSX), are represented by different hatched patterns. Any DSF with $\omega < -3°$ is energetically most unlikely. According to these calculations, any DSF with $-3° < \omega < 4°$ is possible, even for relatively large radii. For a subunit twist larger than 3°, the angle must be positive, and r should not be larger than a limited value, e.g., 80 Å for $\omega = 8°$. The energy difference between a DSF with $\omega = 8°$ and a DSF with $\omega = -8°$ is very large. Fig. 4 *a* thereby demonstrates that HbS fibers with a subunit twist of more than 3° must be right-handed. This is consistent with experimental observations (Dykes et al., 1979; Lewis et al., 1991).

The double strands in the crystal lack a perfect 2_1 screw. It is not clear whether the deviation from 2_1 screw symmetry in the crystal is due to adventitious crystal contacts or to physiologically important intermolecular interactions. A double strand with perfect 2_1 symmetry can be constructed from the averaged coordinates of two HbS molecules in the crystal.

In Fig. 4 *b*, the energy map for an averaged double strand with true 2_1 symmetry between molecule S_0 and T_0 is calculated for comparison with that of the crystal double strand having only approximate 2_1 symmetry (Fig. 4 *a*). Fig. 4 *b* still reflects the handedness of the HbS fiber, but not quite as strongly as Fig. 4 *a*.

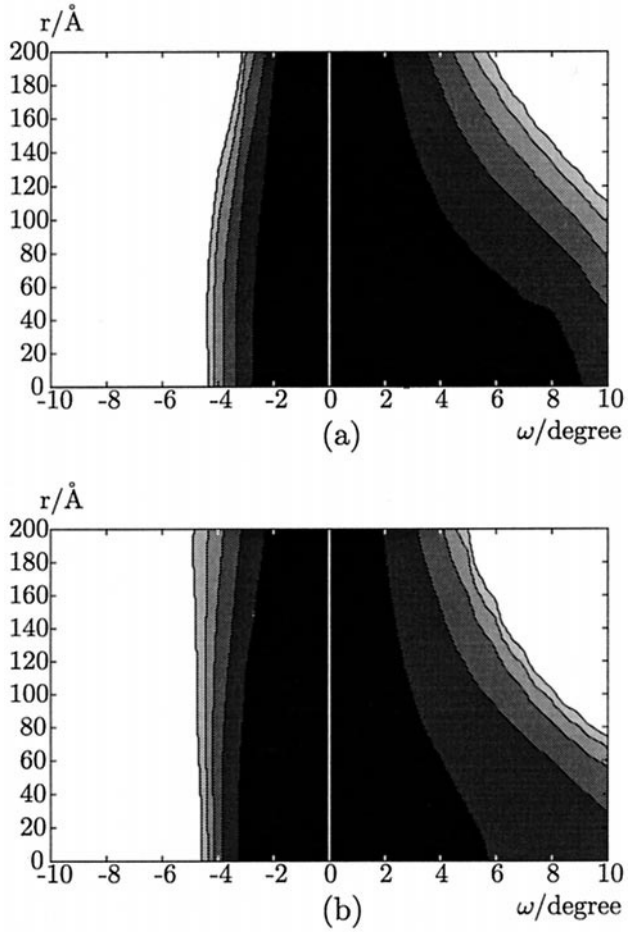

FIGURE 4 (*a*) The contour map of molecular energies within DSF. The five hatched patterns, from dark to light, represent energy levels of $0.9E_x$, $0.8E_x$, $0.7E_x$, $0.6E_x$, and $0.5E_x$, where E_x is the energy within a DSX. Energies outside the hatched regions are higher and are very dependent on β. DSF and the fibers have to be right-handed if the value of the subunit twist is large. (*b*) The corresponding energy map for an averaged double strand with a true 2_1 between the molecules S_0 and T_0, where the residue positions were obtained by averaging over the two molecules in the crystal. (b) is more symmetrical about $\omega = 0$ than is (a), failing to predict the handedness of the HbS fiber.

Axial and lateral interactions within DSF

The transformation method described in the Methods automatically preserves the lateral molecular distances. But the axial distances change with variations in the structural parameters ω, r, and β. It is expected that the axial interactions change with structural parameters in a way that is different from the manner of change of lateral interactions.

The curves of E versus r for lateral interactions, axial interactions, and the sum of the two, of a DSF with $\omega = 8°$, are plotted in Fig. 5. The axial interaction energy increases with increasing r and approaches zero asymptotically. The lateral interaction energy remains constant ($\pm$ 5%) and equal to that of a DSX, for r less than 100 Å, and then increases sharply when $r > 120$ Å.

The variations in axial and lateral interaction energies reflect changes of two kinds in the molecular contacts. The number of axial residue contacts gradually decreases with increasing r, because of stretching of the molecular strand, and the axial interactions accordingly become weaker. Invariance of lateral molecular distances results in consistency of lateral interaction energy over a wide range of r and ω. However, for large r and/or ω, the relative molecular orientations lead to very short residue-to-residue distances in the $\beta 6$ region and preclude the $\beta 6$ contact from being maintained. In this case, the energy calculation results in very high values due to physically impossible molecular interpenetrations.

Limitation of radial distance and subunit twist of DSF

Curves of lateral interaction energies versus r, like those in Fig. 5, can be drawn for various values of ω and β. Both the total and lateral energies are nearly β independent over wide ranges of r and ω. It is more convenient to analyze these energies on a two-dimensional energy map, as shown in Fig. 6 *a*. Inside the hatched area of the map the lateral energy of DSF is within 5% of that of a DSX, and it is larger outside.

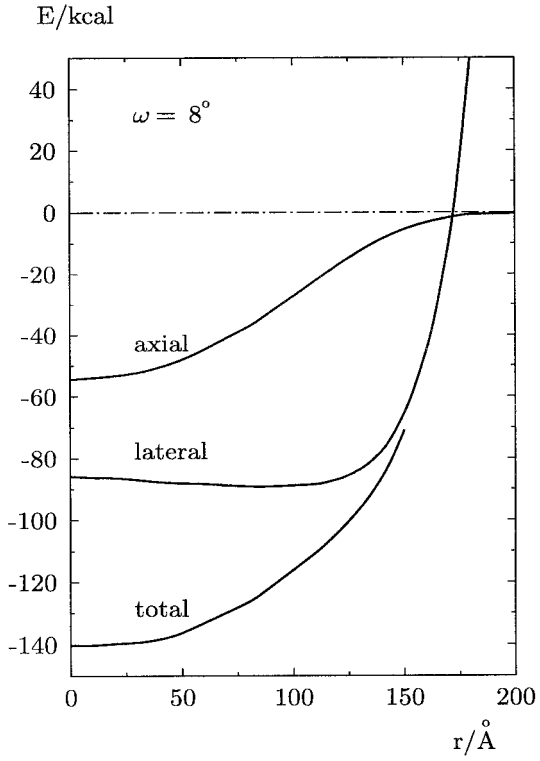

FIGURE 5 The curves of E against r for axial, lateral, and total molecular energies within DSF for a subunit twist of 8°. The axial energy decreases gradually with increasing r and asymptotically approaches zero, whereas the lateral energy remains unchanged before r reaches 90 Å, and increases abruptly afterward.

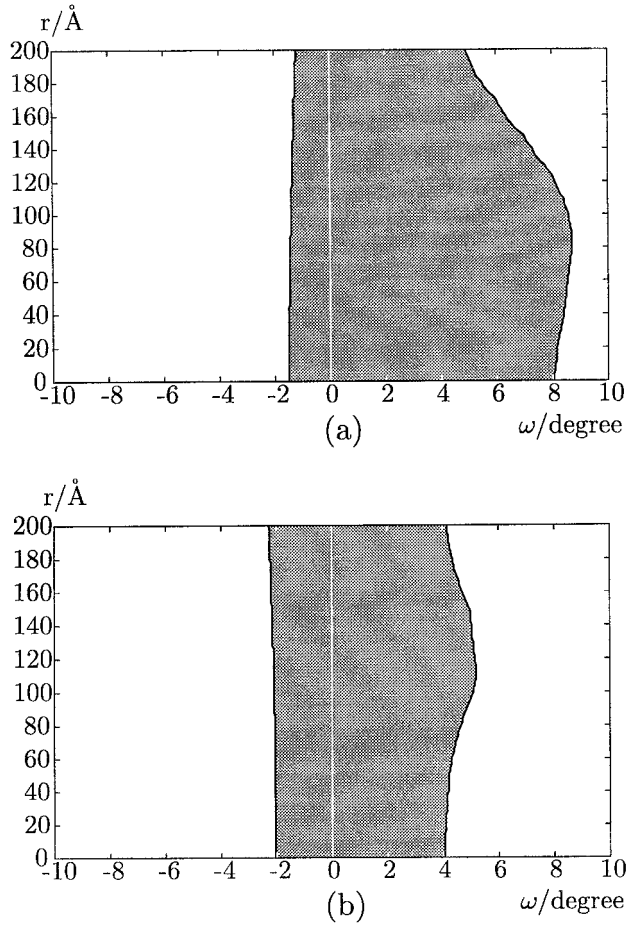

FIGURE 6 (*a*) Energy map for lateral interaction. The dark area represents the region of parameters r and ω of DSF, whose lateral molecular energies are equal to those of DSX within ~5%. The upper right edge of the dark region represents the maximum r for various values of ω. (*b*) The lateral interaction energy for a 2_1-averaged double strand.

The energy in the hatched region can be considered constant, given the approximate nature of the energy calculations. It is well known that the lateral intermolecular interaction, with the participation of β6 Val, is essential for the formation of HbS fiber. Any acceptable model for DSF must possess a lateral energy of interaction adequate to stabilize the fiber. Fig. 6 *a* confirms this issue quantitatively; any viable DSF has approximately the same lateral interaction energy as a DSX. It follows that the hatched regions in Fig. 6 *a* represent those parameters consistent with a stable DSF. The allowed subunit twist is never less than $-1.5°$ or larger than 8°, and the maximum value of r, r_{max}, is ~120 Å for $\omega = 8°$, and increases as ω decreases. The maximum possible radius for a double strand appears to vary linearly with subunit twist, as shown in the upper right-hand part of Fig. 6 *a*. A more complete curve of r_{max} versus ω is shown in Fig. 7, which demonstrates that the relationship is linear over the range of $\omega = 4\sim8°$, but deviates from linear for smaller values of ω. The curve approaches an infinitely large value of r_{max} as ω approaches 0. This corresponds to where the DSF becomes a DSX, and the infinite radius corresponds to the essentially unbounded packing of double strands in the crystal.

The limitations for the parameters r and ω of DSF correspond to the limitations on the radial size and the long axial period of an HbS fiber. The transverse fiber size, R, is larger than r_{max} by an amount approximately equal to the radius of the HbS molecule, i.e., $R \cong r_{max} + 27$ Å, where 27 Å is the radius of an HbS molecule. The curve of ω versus r_{max} is redrawn as a curve of p, the pitch or long period of a helix with angle ω, against r_{max}, as shown in Fig. 7. This curve corresponds closely to the experimental curve of pitch versus radius for various aggregates of sickle cell hemoglobin (Makowski and Magdoff-Fairchild, 1986), which is superimposed on the theoretical curve in Fig. 7.

As shown in Figs. 4 *a* and 6 *a*, the total intermolecular energies, especially the lateral energies, within an HbS double strand may be constant over a very wide range of parameters r and ω. That is why HbS aggregates are so polymorphic, and why a cumulative azimuthal disorder is observed in HbS fibers (Carragher et al., 1988).

The corresponding lateral energy map for a 2_1-averaged double strand is shown in Fig. 6 *b* for comparison. It is not consistent with the variety of fiber forms observed and suggests that the 2_1 model is an inadequate basis for constructing double strands.

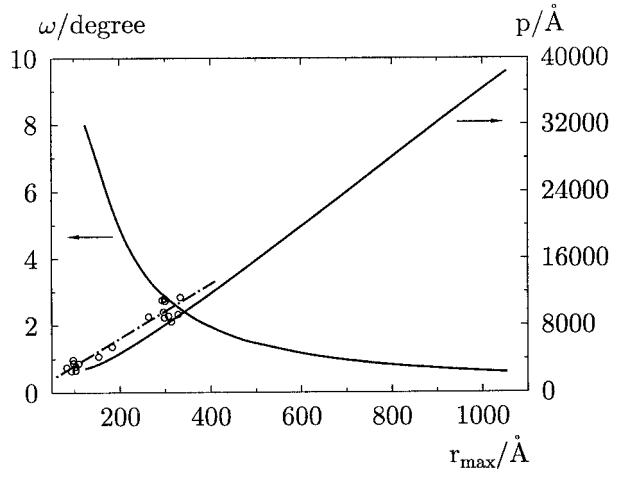

FIGURE 7 The relationship between p, the pitch of the helix, and r_{max}, the maximum allowed radial distance, and the relationship between ω, the subunit twist of helix, and r_{max}. The observed data (○) and the least-squared fitting line with slope of 32.44 (– · –) were taken from Makowski and Magdoff-Fairchild (1986).

Residue contacts within DSF

Two criteria have been used to count residues in contact within an HbS double strand: the 5-Å criterion, in which all residues containing an atom within 5 Å of an atom in a neighboring molecule are considered as those participating in a contact (Wishner et al., 1976; Rosen and Magdoff-Fairchild, 1982); and the sum of van der Waals radii criterion, in which all residues are included as being in contact if they contain an atom whose van der Waals radius overlaps with that of an atom in a neighboring molecule (Padlan and Love, 1985b).

These criteria are not readily applied to the simplified protein representation used here. Although a complete list of atomic coordinates could be reconstructed from the simplified representation, the approximations implicit in the energy calculations do not warrant this level of precision. Consequently, the contact criterion used was as follows. A residue of one molecule is listed as participating in a contact only when its distance from a residue of a neighboring molecule, d_{1-2}, satisfies

$$d_{1-2} < r_2 + r_2 + s$$

where r_1 and r_2 are the radii of the spheres, representing the two residues, and s is an adjustable distance in the analytical approximation formula for computing of the accessible surface area (Wodak and Janin, 1980). For a hard sphere residue, s is equal to 2.8 Å, twice the van der Waals radius of a water molecule. Usually, however, the spheres representing the residues are allowed to penetrate to a small extent, and a smaller s is used. As recommended by Wodak and Janin (1980), 2.5 Å was used in this work. This criterion reflects the fact that a residue of one molecule will contribute to hydrophobic interactions with another molecule, only when it is within d_{1-2} of a residue of the second molecule.

Residues participating in the four kinds of contacts in the DSX and in two different DSF, as defined by this criterion, are listed in Fig. 8. Residue pairs in contact were connected with straight lines. Residues listed in bold make contacts with at least three residues of the neighboring molecule, indicating that they are important for the molecular contact. In all cases, the Val β6 of the β_2 chain makes the most contacts with the lateral adjacent HbS molecule. For the lateral interactions, Thr87 of the β_1 chain is of an importance comparable to that of Val β6.

We compared Fig. 8 *a* with the contact listing provided by 5-Å criterion for double strands with a true 2_1 symmetry in crystalline HbS (Wishner et al., 1976). The listings of axial contacts are identical. It is more difficult to make a comparison for the lateral contacts because of the obvious nonequivalency of the two lateral contacts in Fig. 8 *a*. The main features of lateral contacts are similar in the two listings, with most differences occurring among residues at the edge of the contact zone, and usually making only one contact.

The first and second lateral contacts within DSX involve 36 and 52 residue pairs, respectively, as defined by our simplified molecular representation, and are indicated in Fig. 8 *a*. Padlan and Love (1985b) counted 37 atomic pairs for the first lateral contact and 72 for the second. The contacts in DSFs with parameters ω of 8°, r of 40 Å, and $\beta = 0°$ or 90°, are enumerated in Fig. 8, *b* and *c*. There are 39–40 and 44–45 residue pairs in the first and second lateral contacts, respectively. Surprisingly, the two lateral contacts are more symmetrical in these helical structures than in the crystal. Pointing out the nonequivalence of the two contacts in crystalline HbS, Padlan and Love (1985b) suggested that "if the two lateral contacts are made equivalent . . . , then a helical double strand would be produced."

The number of residue contacts varies as a function of the radial distance of DSF from the fiber axis, as shown in Fig. 9 for $\omega = 8°$ and $\beta = 90°$. The number of axial contacts decreases with increasing r as expected, because of the stretching of the double strand, whereas lateral contacts change little over the range $r = 0 \sim 80$ Å. When $r > 100$ Å, the number of lateral contacts increases, as shown by the dotted line in Fig. 9. But most of these are forbidden interactions, because of intermolecular interpenetration that forces the intermolecular interaction energy to become positive. We examined distances between residues from two lateral adjacent molecules for the DSF. Some of these distances decrease with increasing r when $r > 80$ Å, and eventually form forbidden overlaps as the value of r becomes even larger. It is these forbidden interpenetrations in the β6 contact region that are responsible for restricting the transverse size of the HbS fiber for a given ω.

From the above results we conclude that the major factor forming and stabilizing an HbS double strand in the crystal or in any of the observed helical structures is the β6 contacts. The major factor limiting transverse size of any structure, comprising HbS double strands, is close contacts in the β6 region that preclude the maintenance of the β6 contact

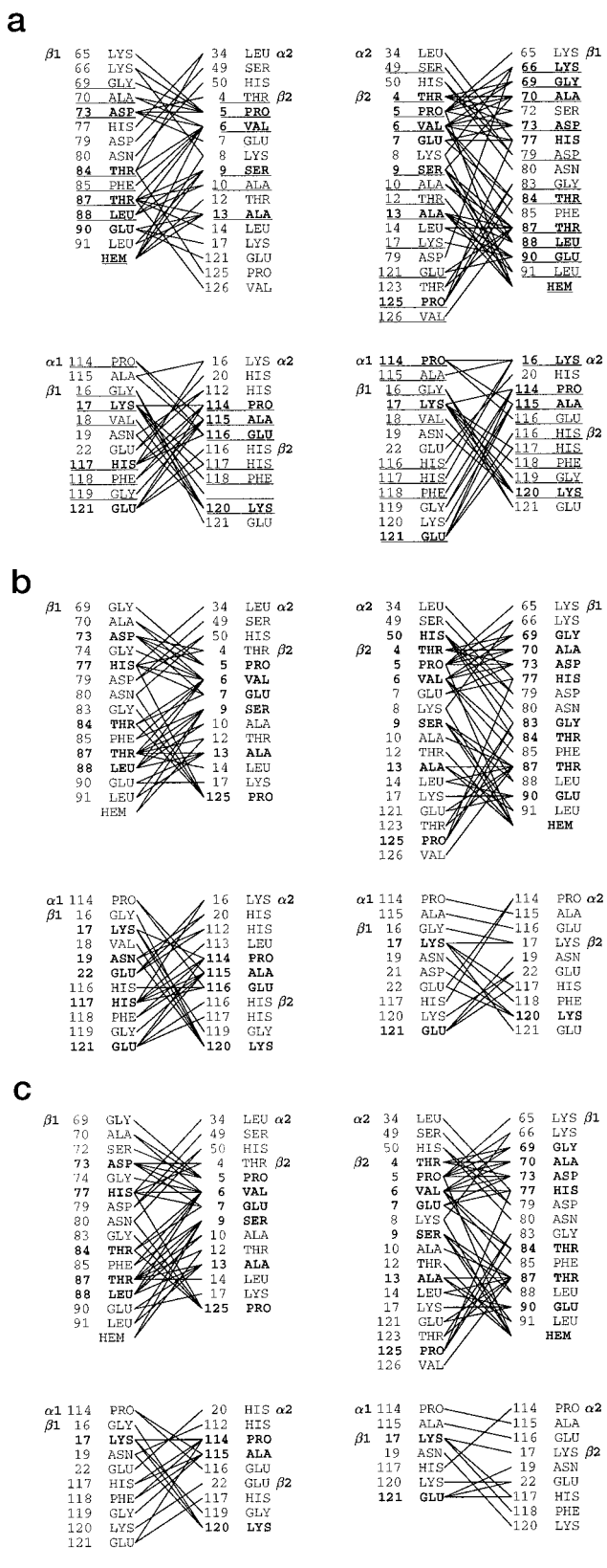

FIGURE 8 Listing of the residues participating in molecular contacts in (*a*) DSX; (*b*) DSF with $\omega = 8°$, $r = 40$ Å, and $\beta = 0°$; (*c*) DSF with $\omega = 8°$, $r = 40$ Å, and $\beta = 90°$. A residue is listed here when the distance from it to a residue in a neighboring molecule is equal to or less than a special value. This value is a sum of the radii of the two spheres representing the two related residues in the simplified protein model, plus 90% of the van der Waals diameter of a water molecule. The upper left, upper right, lower left, and lower right charts in each figure represent the molecular interactions of S_0-T_0, S_0-T_{-1}, S_0-S_1, and T_0-T_1, respectively. The residues, the names of which are printed in bold, are important for the molecular contact. They make contacts with at least three residues of a neighboring molecule. The residue valine, $\beta 6$ of the β_2 chain, makes the most contacts with a laterally adjacent molecule in all cases. The listing is based on a simplified protein model in which the residue is replaced by a sphere. The number of residues in molecular contacts is probably overestimated. A comparison is made with a listing of residues in contact, based on atomic coordinates (marked with *underlines* in *a*), in HbS crystal (Padlan and Love, 1985b).

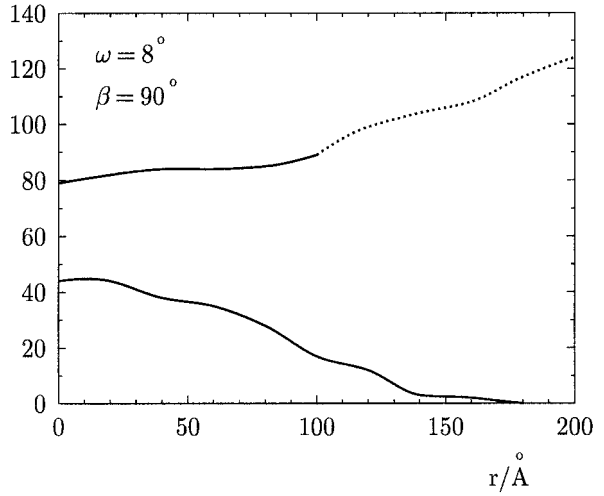

FIGURE 9 The number of lateral contacts (*upper curve*) and axial contacts (*lower curve*) plotted against r for $\omega = 8°$ and $\beta = 90°$. The number of axial contacts decreases with increasing r, as expected. The number of lateral contacts, however, increases with increasing r, because of the formation of forbidden interpenetrations of adjacent molecules.

for certain pairs of r and ω. The axial interactions decrease gradually with radial growth of the HbS helical structure, as shown in Figs. 5 and 9 of this paper, and figure 3 of Watowich et al. (1989). Although the loss of axial interactions may be compensated for by formation of new inter-double-strand interactions and entropy gain in higher radius double strands, for any given ω, at some r_{max} forbidden molecular interpenetrations in the $\beta 6$ contact region will preclude further radial growth of the fiber.

Orientation of molecular axis of DSF

Polarized absorption measurements have placed a critical constraint on models for HbS fibers by determining that the angle between the molecular axis and the fiber axis must not be larger than 22° (Hofrichter et al., 1973). The molecular orientation angles of the two HbS molecules in DSF, transformed from DSX to DSF by the transformation method described above, were calculated over the entire range of β angles, over radial distances from 0 to 200 Å, and with a fixed subunit twist $\omega = 8°$. These results are summarized in Fig. 10,

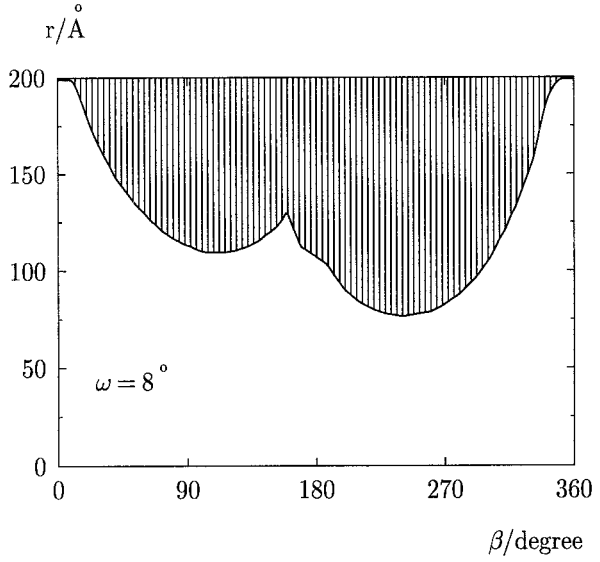

FIGURE 10 Map of the allowed values of parameters r and β for DSF with subunit twist of 8°. When parameters r and β of a DSF fall in the shadow region, at least one molecule of the double strand possesses an orientation angle that is larger than 22°, in contradiction to the experimental observations.

in which the shaded region is forbidden because at least one molecule of the DSF possesses an orientation angle larger than 22°. As shown in the figure, any DSF with $r < 80$ Å has molecular orientation angles consistent with observations.

Molecular stagger in DSF

The molecular stagger, defined as the axial spacing (along the fiber axis) between the two representative molecules in a DSF (e.g., S_0 and T_0), changes with variations in structural parameters ω, r, and β. The curves of h, molecular stagger, versus β for $\omega = 8°$ are shown in Fig. 11, where the dotted line is for $r = 50$ Å and the solid line is for $r = 90$ Å. The axial distance from S_0 to S_1 is always 64 Å. So, if the stagger between S_0 and T_0 is 32 Å $- \Delta$, the stagger between T_0 and S_1 is 32 Å $+ \Delta$. In the crystals the stagger is always 32 Å. Deviation of the stagger in DSF from 32 Å is an unavoidable consequence of the consistency of the lateral molecular distance. The stagger may also be calculated from the double-strand tilting (Lewis et al., 1994).

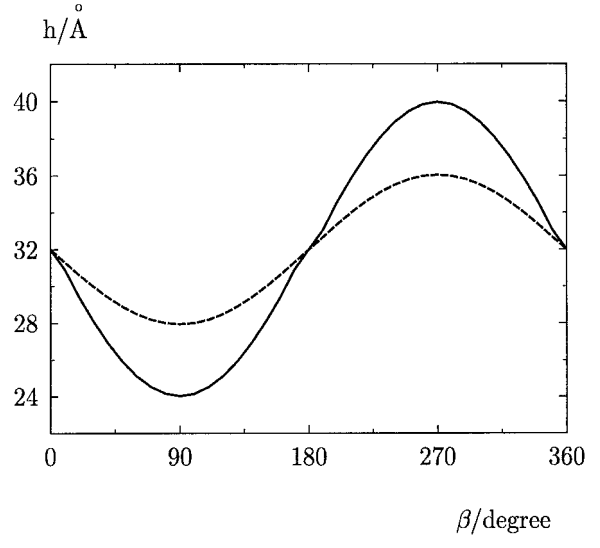

FIGURE 11 The curves of h, molecule staggers, against β for $\omega = 8°$ and $r = 50$ Å (– – –), and $r = 90$ Å (——). In the crystal the stagger is a constant, 32 Å. In a fiber it changes with variation of structural parameters ω, r, and β.

In this study, helical HbS double strands have been constructed in a wide range of structural parameters, including all of the observed polymorphic aggregates of HbS. The assumptions made in this construction were that the HbS molecules can be considered rigid; that the β6 contact distance (lateral contact distance) is kept constant during the transformation from a crystalline double strand to a fiber double strand; that the relative orientation between lateral adjacent molecules is set as half of the subunit twist; and that the subunit rise (along the fiber axis) is constant at 64 Å, as indicated by x-ray diffraction data. The stability of HbS double strands has been analyzed by using these models.

The properties of the helical double strands constructed in this way are consistent with the observed properties of the known aggregates of HbS. The contact of Val β6 of the β_2 chain of hemoglobin S is of paramount importance in the stability of all of the model double strands constructed. The energetics of the constructed models correctly predict the limiting diameter of the physiologically relevant seven double-strand fibers, the handedness of these fibers, and the molecular orientations within these fibers. Furthermore, the molecular origins of these effects can be mapped to specific substructures in the HbS molecules by using these models.

The approximate method of energy calculation, developed by Janin and co-workers, was applied in the docking problem. When the structure of a protein-protein complex was predicted, several candidate models were selected by this technique. The selection of candidate solutions is the first and critical step of the whole docking procedure. The Wodak-Janin technique performs no worse than others in which a full atomic description is used, and more energy terms, including ionic interactions, hydrogen bonds, etc., are involved (Strynadka et al., 1996; Chefils et al., 1991).

The assumption made in the approximation about the omission of ionic interaction and hydrogen bonds worked well for the interactions within the HbS double strand. It is well known that in crystalline HbS there are 281 atomic pairs for interactions within a HbS double strand. Only one of them is ionic, and 10 are potential hydrogen bonds. In other words, more than 96% of molecular interactions within the double strand are hydrophobic. In contrast, in the protein-protein complexes tested by Janin, about one-third of residue contacts are hydrogen bonds.

This technique, however, cannot be used to obtain the absolute value of molecular interaction energy.

To calculate interaction energies within DSF accurately, a full atomic description of HbS molecules should be used, and all energy terms, including ionic interactions, H-bonds, and interaction with water molecules, should be taken into consideration. The method of transformation of DSX into DSF that we have developed in this paper can provide initial values of molecular positions and molecular orientations within a DSF for these energy calculations.

The method developed in this paper cannot predict the conditions under which the various aggregates form, because it does not consider the interactions among the double strands. A complete model for the HbS fiber, including all interactions among the double strands, can now be built by using as the building blocks the double strands constructed here. That model will allow a complete enumeration of the interactions among HbS molecules in the fiber.

APPENDIX

Calculation of the position of molecule T_0

The mass centers of the molecules S_0, T_0, and S_1 of a DSX were located at s_0, t_0, and s_1 in the fiber reference system XYZ as shown in Fig. 12 *a*, where the intermolecular distance s_0t_0 is equal to that of t_0s_1. After a helical rotation by the subunit twist ω, the molecules T_0 and S_1 are moved to t_0' and s_1' respectively, leaving the molecule S_0 at s_0 as a reference point. The points s_0, s_1, and s_1' are on the surface of cylinder S with a radius of R_s, equal to the distance between molecule S_0 and the fiber axis. The points t_0 and t_0' are on the surface of cylinder T with a radius of R_t. After this rotation t_0' is usually not equidistant from s_0 and s_1'. To satisfy restraint (2), the center of molecule T_0 must be moved from t_0' to t_0'' on the surface of cylinder T to have $s_0t_0'' = t_0''s_1 = d$, the expected lateral molecule distance in a DSX.

The coordinates of the centers of molecules T_0 and S_1 in DSF, or of the points t_0'' and s_1' in Fig. 12 *a*, were derived in a cylindrical reference system. The fiber system in Fig. 12 *a* was adjusted so that the coordinates of point s_0 become $(R_s, 0, 0)$. And accordingly, those of points t_0 and s_1'' in the same system are (R_t, α, h) and (R_s, ω, a), respectively, where ω is the subunit twist and a is the subunit rise. R_s and R_t, the radial distances of two molecular strands, are determined uniquely by the structural parameters r and β. α and h are related explicitly to r, β, and the subunit twist ω:

$$h = \frac{a}{2} - \frac{2B}{a}\sin(\alpha - \omega/2) \tag{A1}$$

$$a = \arccos P + \omega/2 \tag{A2}$$

where

$$B = R_sR_t\sin(\omega/2) \tag{A3}$$

$$P = \frac{a^2}{4B}\left\{\sqrt{\cot^2\frac{\omega}{2} + \frac{4R_t^2}{a^2} + \frac{4R_s^2}{a^2} + 1 + \frac{16B^2}{a^4} - \frac{4d^2}{a^2}} - \cot\frac{\omega}{2}\right\} \tag{A4}$$

Usually we have two solutions for h and α, and one closer to t_0' in Fig. 12 *a* is chosen as the final solution. When r and/or ω are large and β is close to 0° or 180°, a small adjustment (less than 0.4 Å) of R_t is needed to guarantee the existence of the solutions for h and α.

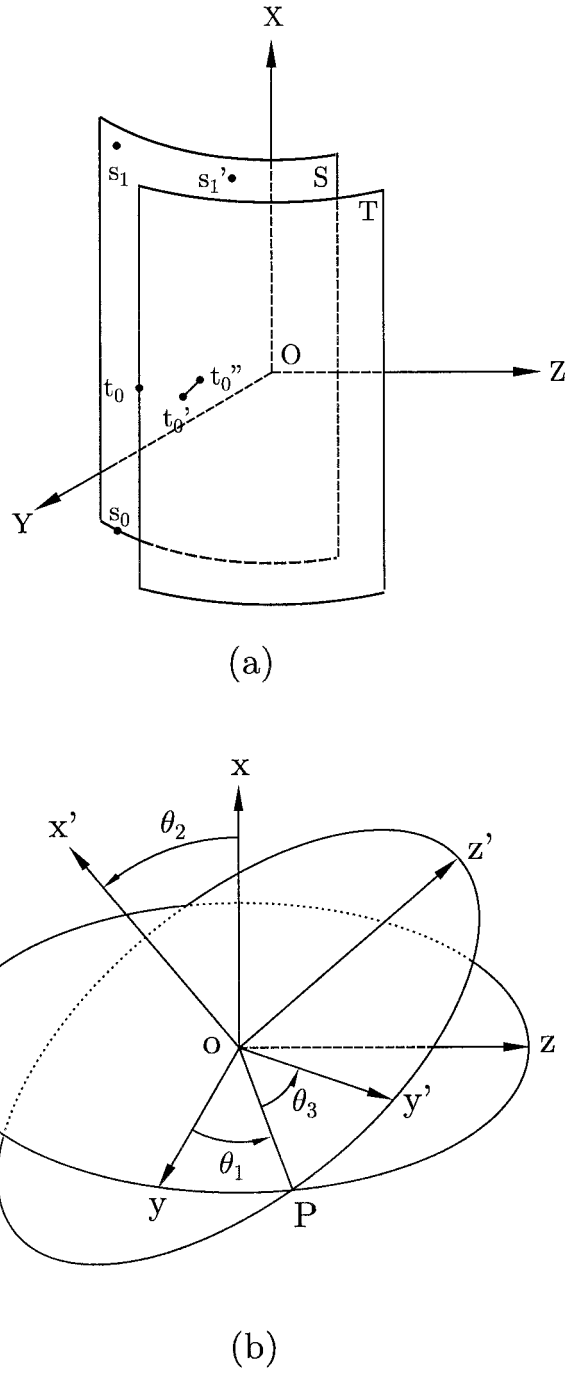

FIGURE 12 (*a*) Position of molecule T_0 in DSF. (*b*) The two local reference systems with Eulerian angles.

It is easy to convert the coordinates of points t_0'' and s_1' in the cylindrical system, (R_s, ω, a) and (R_t, α, h), to those in a Cartesian local system in Fig. 12 *a*. They are (x_2, y_2, z_2) and (x_3, y_3, z_3), respectively.

Eulerian angles

It is convenient to discuss the rotations of a reference system in terms of Eulerian angles instead of those of a rigid body. Two local reference systems with a common origin, xyz and $x'y'z'$, are shown in Fig. 12 *b*. The mass centers of the deformed double strand are placed on plane xoy, with

molecule S_1 on the axis ox. Three points of the target are on plane $x'oy'$, with s_1' on the axis ox'.

As shown in Fig. 12 *b*, the rotations of reference system o-xyz to o-$x'y'z'$ consist of a rotation by θ_1, contained between oy and oP, about the axis ox; a rotation by θ_2, contained between ox and ox', about the vector oP; and a rotation by θ_3, contained between oP and oy', about the axis ox'. The values of the angles may be obtained from the directional cosines of their starting and end vectors. The directional cosines of ox, oy and ox' are (1, 0, 0), (0, 1, 0) and $(x_3/L, y_3/L, z_3/L)$, respectively, where (x_3, y_3, z_3) are the coordinates of point s_1', and L is the length os_1'.

The directional cosines of vectors oP and oy' could be obtained from equations of related planes. The equation of plane yoz is simple:

$$x = 0 \tag{A5}$$

The equation of plane $y'oz'$, passing through the origin and perpendicular to the axis ox', is

$$xx_3 + yy_3 + zz_3 = 0 \tag{A6}$$

The equation of the vector oP, the common line of plane yoz and $y'oz'$, is then expressed in canonical form:

$$\frac{x}{0} = \frac{y}{-z_3} = \frac{z}{y_3} \tag{A7}$$

The equation of plane $x'oy'$, passing through three points o (0, 0, 0), t_0'' (x_2, y_2, z_2), and s_1' (x_3, y_3, z_3), is

$$x(y_3z_2 - y_2z_3) + y(z_3x_2 - z_2x_3) + z(x_3y_2 - x_2y_3) = 0 \tag{A8}$$

The canonical form of the equation of axis oy', the common line of plane $x'oy'$ and plane $y'oz'$, is

$$\frac{x}{1} = \frac{y}{m} = \frac{z}{n} \tag{A9}$$

where

$$\begin{cases} 1 = z_3(z_3x_2 - z_2x_3) - y_3(x_3y_2 - x_2y_3) \\ m = x_3(x_3y_2 - x_2y_3) - z_3(y_3z_2 - y_2z_3) \\ n = y_3(y_3z_2 - y_2z_3) - x_3(z_3x_2 - z_2x_3) \end{cases} \tag{A10}$$

Equations A7 and A9 give the directional cosines of ${}_0P$ and ${}_0y'$ as $(0, -z_3, y_3)$ and (l, m, n), respectively.

The Eulerian angles are given by the equations of their initial and final vectors as follows:

$$|\theta_1| = \arccos\left(\frac{-z_3}{\sqrt{y_3^2 + z_3^2}}\right) \tag{A11}$$

$$|\theta_2| = \arccos\left(\frac{x_3}{\sqrt{x_3^2 + y_3^2 + z_3^2}}\right) \tag{A12}$$

$$|\theta_3| = \arccos\left(\frac{ny_3 - mz_3}{\sqrt{(l^2 + m^2 + n^2)(y_3^2 + z_3^2)}}\right) \tag{A13}$$

The direction of the angle depends on the handedness of the system, comprising the rotating axis, and initial and final vectors. It is positive for a right-handed system and negative for a left-handed system. Finally, we have

$$\theta_1 = \begin{cases} |\theta_1|, & \text{when } y_3 \geq 0 \\ -|\theta_1|, & \text{when } y_3 < 0 \end{cases} \tag{A14}$$

$$\theta_2 = |\theta_2| \tag{A15}$$

$$\theta_3 = \begin{cases} |\theta_3|, & \text{when } l \geq 0 \\ -|\theta_3|, & \text{when } l < 0 \end{cases} \tag{A16}$$

θ_2 is special because it has a different range, $0 \leq \theta_2 \leq \pi$.

The matrix for the rotation of the deformed double-strand is then

$$M = \begin{bmatrix} \text{C2} & \text{S2S3} & \text{C2S2} \\ \text{S1S2} & \text{C1C3} - \text{C2S1S3} & -\text{C1S3} - \text{C2C3S1} \\ \text{C1S2} & \text{C3S1} + \text{C1C2S3} & -\text{S1S3} + \text{C1C2C3} \end{bmatrix} \tag{A17}$$

where C and S indicate cos and sin, respectively, and 1, 2, and 3 indicate θ_1, θ_2, and θ_3, respectively.

This work was supported by the National Institutes of Health (grant HL 28381) and a grant from the National Science Foundation.

REFERENCES

Bernstein, F. C., T. F. Koetzle, G. J. B. Williams, E. F. Meyer, M. D. Brice, J. R. Rodgers, O. Kennard, T. Shimanouchi, and M. Tasumi. 1977. The Protein Data Bank: a computer-based archival file for macromolecules and structures. *J. Mol. Biol.* 112:535–542.

Bluemke, D. A., B. Carragher, M. J. Potel, and R. Josephs. 1988. Structural analysis of polymers of sickle cell hemoglobin. II. Sickle hemoglobin macrofibers. *J. Mol. Biol.* 199:333–348.

Carragher, B., D. A. Bluemke, B. Gabriel, M. J. Potel, and R. Josephs. 1988. Structural analysis of polymers of sickle cell hemoglobin. I. Sickle hemoglobin fibers. *J. Mol. Biol.* 199:315–331.

Chefils, J., S. Duquerroy, and J. Janin. 1991. Protein-protein recognition analyzed by docking simulation. *Protein Struct. Funct. Genet.* 11: 271–280.

Cretegny, I., and S. J. Edelstein. 1993. Double strand packing in hemoglobin S fibers. *J. Mol. Biol.* 230:733–738.

Dykes, G. W., R. H. Crepeau, and S. J. Edelstein. 1979. Three-dimensional reconstruction of the 14-filament fibers of hemoglobin S. *J. Mol. Biol.* 130:451–472.

Eaton, W. A., and J. Hofrichter. 1990. Sickle cell hemoglobin polymerization. *Adv. Protein Chem.* 40:63–280.

Edelstein, S. J. 1981. Molecular topology in crystals and fibers of hemoglobin S. *J. Mol. Biol.* 150:557–575.

Hofrichter, J., D. G. Hendricker, and W. A. Eaton. 1973. Structure of hemoglobin S fibers: optical determination of the molecular orientation in sickled erythrocytes. *Proc. Natl. Acad. Sci. USA.* 70:3604–3608.

Levitt, M. 1976. A simplified representation of protein conformations for rapid simulation of protein folding. *J. Mol. Biol.* 104:59–107.

Lewis, M. R., L. J. Gross, and R. Josephs. 1994. Cryo-electron microscopy of deoxy-sickle hemoglobin fibers. *Microsc. Res. Tech.* 27:459–467.

Lewis, M. R., T. E. Lee, and R. Josephs. 1991. The hand of the helix of deoxyhemoglobin S fibers. *J. Struct. Biol.* 107:196–199.

Magdoff-Fairchild, B., and C. C. Chiu. 1979. X-ray diffraction studies of fibers and crystals of deoxygenated sickle cell hemoglobin. *Proc. Natl. Acad. Sci. USA.* 76:223–226.

Magdoff-Fairchild, B., L. S. Rosen, and C. C. Chiu. 1982. Triclinic crystals associated with fiber of deoxygenated sickle hemoglobin. *EMBO J.* 1:121–126.

Makowski, L., and B. Magdoff-Fairchild. 1986. Polymorphism of sickle cell hemoglobin aggregates: structural basis for limited radial growth. *Science.* 234:1228–1231.

McDade, W. A., B. Carragher, C. A. Miller, and R. Josephs. 1989. On the assembly of sickle hemoglobin fascicles. *J. Mol. Biol.* 206:637–649.

Padlan, E. A., and W. E. Love. 1985a. Refined crystal structure of deoxy hemoglobin S. I. Restrained least-squares refinement at 3.0 Å resolution. *J. Biol. Chem.* 260:8272–8279.

Padlan, E. A., and W. E. Love. 1985b. Refined crystal structure of deoxy hemoglobin S. II. Molecular interactions in the crystal. *J. Biol. Chem.* 260:8280–8291.

Potel, M. J., T. E. Wellems, R. J. Vassar, B. Deer, and R. Josephs. 1984. Macrofiber structure and the dynamics of sickle cell hemoglobin crystallization. *J. Mol. Biol.* 177:819–839.

Rosen, L. S., and B. Magdoff-Fairchild. 1982. Molecular packing in a second monoclinic crystal of deoxygenated sickle hemoglobin. *J. Mol. Biol.* 157:181–189.

Sharp, K. A., A. Nicholls, R. F. Fine, and B. Honig. 1991. Reconciling the magnitude of the microscopic and macroscopic hydrophobic effects. *Science.* 252:106–109.

Strynadka, N. C. J., M. Eisenstein, E. Katchalki-Katzir, B. K. Shoichet, I. D. Kuntz, R. Abagyan, M. Totrov, J. Janin, J. Cherfils, F. Zimmermen, A. Olson, B. Duncan, M. Rao, R. Jackson, M. Sternberg, and M. N. G. James. 1996. Molecular docking programs successfully predict the binding of a β-lactamase inhibitory protein to TEM-1 β-lactamase. *Nature Struct. Biol.* 3:233–239.

Watowich, S. J., L. J. Gross, and R. Josephs. 1989. Intermolecular contacts within sickle hemoglobin fibers. *J. Mol. Biol.* 209:821–828.

Watowich, S. J., L. J. Gross, and R. Josephs. 1993. Analysis of the intermolecular contacts within sickle hemoglobin fibers: effect of site-specific substitutions, fiber pitch and double-strand disorder. *J. Struct. Biol.* 111:161–179.

Wellems, T. E., and R. Josephs. 1980. Helical crystals of sickle cell hemoglobin. *J. Mol. Biol.* 137:443–450.

Wishner, B. C., J. C. Hanson, W. M. Ringle, and W. E. Love. 1976. Crystal structure of sickle-cell deoxyhemoglobin. *In* Proceedings of the Symposium on Molecular and Cellular Aspects of Sickle Cell Disease, publication (NIH) 76-1007. J. I. Hercules, G. L. Cottam, M. R. Waterman, and A. N. Schechter, editors. Department of Health and Human Services, NIH, Bethesda, MD. 1–29.

Wishner, B. C., K. B. Ward, E. E. Lattman, and W. E. Love. 1975. Crystal structure of sickle-cell deoxyhemoglobin at 5 Å resolution. *J. Mol. Biol.* 98:179–194.

Wodak, S. J., and J. Janin. 1978. Computer analysis of protein-protein interaction. *J. Mol. Biol.* 124:323–342.

Wodak, S. J., and J. Janin. 1980. Analytical approximation to the accessible surface area of proteins. *Proc. Natl. Acad. Sci. USA.* 77:1736–1740.